

## Accelerated Publications

---

### Phenylalanine Residues in the Active Site of Tyrosine Hydroxylase: Mutagenesis of Phe300 and Phe309 to Alanine and Metal Ion-Catalyzed Hydroxylation of Phe300<sup>†</sup>

Holly R. Ellis,<sup>‡,§</sup> S. Colette Daubner,<sup>‡,§</sup> Ruth I. McCulloch,<sup>||</sup> and Paul F. Fitzpatrick<sup>\*,‡,||</sup>

Department of Biochemistry and Biophysics and Department of Chemistry, Texas A&M University, College Station, Texas 77843-2128

Received May 20, 1999; Revised Manuscript Received June 30, 1999

**ABSTRACT:** Residues Phe300 and Phe309 of tyrosine hydroxylase are located in the active site in the recently described three-dimensional structure of the enzyme, where they have been proposed to play roles in substrate binding. Also based on the structure, Phe300 has been reported to be hydroxylated due to a naturally occurring posttranslational modification [Goodwill, K. E., Sabatier, C., and Stevens, R. C. (1998) *Biochemistry* 37, 13437–13445]. Mutants of tyrosine hydroxylase with alanine substituted for Phe300 or Phe309 have now been purified and characterized. The F309A protein possesses 40% less activity than wild-type tyrosine hydroxylase in the production of DOPA, but full activity in the production of dihydropterin. The F300A protein shows a 2.5-fold decrease in activity in the production of both DOPA and dihydropterin. The  $K_{6\text{-MPH}_4}$  value for F300A tyrosine hydroxylase is twice the wild-type value. These results are consistent with Phe309 having a role in maintaining the integrity of the active site, while Phe300 contributes less than 1 kcal/mol to binding tetrahydropterin. Characterization of Phe300 by MALDI-TOF mass spectrometry and amino acid sequencing showed that hydroxylation only occurs in the isolated catalytic domain after incubation with a large excess of 7,8-dihydropterin, DTT, and  $\text{Fe}^{2+}$ . The modification is not observed in the untreated catalytic domain or in the full-length protein, even in the presence of excess iron. These results establish that hydroxylation of Phe300 is an artifact of the crystallography conditions and is not relevant to catalysis.

Tyrosine hydroxylase (TyrH)<sup>1</sup> catalyzes the hydroxylation of tyrosine to dihydroxyphenylalanine (DOPA, Scheme 1).

<sup>†</sup> This research was supported in part by NIH Grant GM 47291 and Robert A. Welch Foundation Grant A-1245.

\* Address correspondence to this author at the Department of Biochemistry and Biophysics, Texas A&M University, College Station, TX 77843-2128. Phone: 409-845-5487. Fax: 409-845-9274. E-mail: fitzpat@tamu.edu.

<sup>‡</sup> Department of Biochemistry and Biophysics.

<sup>§</sup> These authors contributed equally to this work.

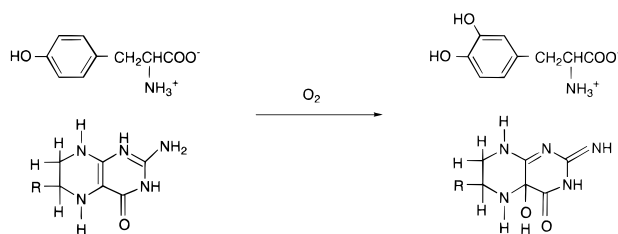
<sup>||</sup> Department of Chemistry.

<sup>1</sup> Abbreviations: DOPA, dihydroxyphenylalanine; IPTG, isopropyl  $\beta$ -D-thiogalactopyranoside; TyrH, tyrosine hydroxylase; PheH, phenylalanine hydroxylase; TrpH, tryptophan hydroxylase; MALDI-TOF, matrix-assisted laser desorption ionization time-of-flight; 6-MPH<sub>4</sub>,

This is the rate-limiting step in the biosynthesis of catecholamine neurotransmitters, and defects in neurotransmitter biosynthesis have been implicated in various neurological disorders (1). TyrH is a homotetramer that belongs to a family of closely related pterin-dependent enzymes which includes tryptophan hydroxylase (TrpH) and phenylalanine hydroxylase (PheH). All three are non-heme iron-containing enzymes that catalyze the hydroxylation of aromatic amino acids utilizing tetrahydrobiopterin as the reducing substrate.

6-methyltetrahydropterin; DTT, dithiothreitol; DHPR, sheep dihydropterin reductase;  $K_{\text{Tyr}}$ ,  $K_M$  value for tyrosine;  $K_{6\text{-MPH}_4}$ ,  $K_M$  value for 6-methyltetrahydropterin; LB-carb, Luria–Bertani broth with 100  $\mu\text{g}/\text{mL}$  carbenicillin.

Scheme 1



Sequence analyses and proteolysis experiments have shown that enzymes belonging to this family have a common C-terminal catalytic domain and divergent N-terminal regulatory domains (2, 3). Truncates of rat PheH and TyrH lacking the regulatory domains possess full activity (4).

The three-dimensional structure of the catalytic domain of TyrH has been determined with and without 7,8-dihydrobiopterin bound (5, 6). The active site consists of a 17 Å deep cleft at the center of an  $\alpha$ -helical basket. The cleft is lined primarily by four  $\alpha$ -helices, with the iron atom located within the cleft 10 Å below the enzyme surface. Based on this structure and on sequence comparisons of the pterin-dependent hydroxylases, several conserved amino acid residues can be identified in the active site of TyrH (Figure 1). Among these residues, Phe300 and Phe309 are found on the surface of the active site with the side chains directed toward the iron [Figure 1 (5, 6)]. In the recently described structure of the catalytic domain of TyrH with 7,8-dihydrobiopterin bound, an unexpected area of electron density was described on carbon 3 of the aromatic ring of Phe300; this added density was interpreted as a hydroxyl group. In addition, purified TyrH was reported to have a molecular mass 11–16 units higher by mass spectrometry than predicted from the cDNA sequence (6). The hydroxyl group on Phe300 was within hydrogen bonding distance of the main-chain carbonyl of Gln310, leading to the proposal that the role of the hydroxyl was to position Phe300 for proper pterin binding. The unexpected modification of Phe300 was attributed to an autocatalytic process which occurred during expression of the recombinant protein. If such a modified phenylalanine occurs naturally in TyrH, it would join a growing number of modified aromatic amino acid residues which have been found in oxidative enzymes, including quinoproteins and galactose oxidase (7–9). In this report we describe studies of the roles of these conserved phenylalanine residues in TyrH and especially the hydroxylated Phe300. Site-directed mutagenesis has been used to replace Phe300 and Phe309 with alanine, and the resulting proteins have been characterized.

## EXPERIMENTAL PROCEDURES

**Materials.** Oligonucleotides were synthesized on an Applied Biosystems Model 380B DNA synthesizer by the Gene Technology Laboratory of Texas A&M University. 6-Methyltetrahydropterin was purchased from B. Schircks Laboratories. 7,8-Dihydrobiopterin was prepared from tetrahydrobiopterin by the method of Mager et al. (10). Leupeptin, pepstatin, and catalase were obtained from Boehringer Mannheim Corp. Restriction endonucleases *Syl*I and *Fsp*I were from New England Biolabs Inc. TPCK-treated trypsin was purchased from Worthington. Dihydropterin reductase (DHPR) and NADH were from Sigma Chemical Co. *Pfu*

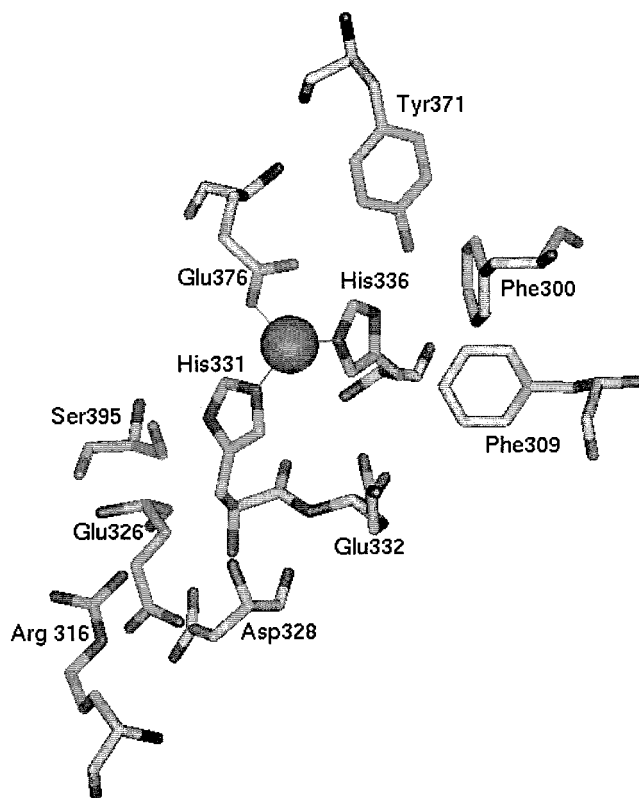


FIGURE 1: Conserved residues in the active site of TyrH. The figure was constructed using the PDB file 1TOH.

DNA polymerase was obtained from Stratagene USA. Phage M13KO7 was from Pharmacia Biotech Inc. Plasmids were purified using kits from Qiagen Inc. *E. coli* strain CJ236 was obtained from Invitrogen Corp. and was used for the production of single-stranded uridine-containing DNA. DNA sequencing was done by the Gene Technology Laboratory of Texas A&M University.

**Vectors for Enzyme Expression.** Site-directed mutagenesis was carried out according to the protocol of Kunkel et al. (11) for the F300A mutation, using the oligonucleotide 5'-gtccg cccgt gatgc cttgg ccagt ctgg-3'. The Stratagene QuikChange kit was used for the F309A mutation, with the oligonucleotide 5'-gcctt ccgtg ttgcg caatg cacc-3'. Plasmid pETYH8 has been previously described (4) and was used as the template for mutagenesis using either method. Mutated plasmids were detected by electrophoretic analysis of restriction digests of plasmids, using *Syl*I for F300A and *Fsp*I for F309A. Following this, the entire coding regions were sequenced to confirm the desired mutations and to detect unexpected mutations. The correct plasmids were named pETYHF300A and pETYHF309A.

**Bacterial Cell Growth.** Plasmids were introduced into competent *E. coli* BL21(DE3) cells and stored as 15% glycerol stocks at  $-80^{\circ}\text{C}$ . Cells from frozen stocks were streaked onto LB-agar plates containing 100  $\mu\text{g/mL}$  carbenicillin for use no earlier than 1 week before growth in liquid culture. Bacteria were grown in LB medium containing 100  $\mu\text{g/mL}$  carbenicillin (LB-carb). One isolated colony of BL21(DE3) containing either pETYHF300A or pETYHF309A was used to inoculate small cultures of LB-carb which were incubated overnight at  $37^{\circ}\text{C}$ . These were used to inoculate 1 L cultures of LB-carb. When the  $A_{600}$  value of the pETYHF300A culture reached 0.6, the flasks were moved

Table 1: Steady-State Kinetic Parameters of Phenylalanine Mutants of Tyrosine Hydroxylase

enzyme	$K_{6\text{-MPH}_4}$ ( $\mu\text{M}$ )	$K_{\text{Tyr}}$ ( $\mu\text{M}$ )	DOPA formation <sup>a</sup>			tetrahydropterin oxidation <sup>b</sup>		
			$V/K_{6\text{-MPH}_4}$ ( $\mu\text{M}^{-1} \text{min}^{-1}$ )	$V/K_{\text{Tyr}}$ ( $\mu\text{M}^{-1} \text{min}^{-1}$ )	$V_{\text{max}}$ ( $\text{min}^{-1}$ )	$V/K_{6\text{-MPH}_4}$ ( $\mu\text{M}^{-1} \text{min}^{-1}$ )	$V/K_{\text{Tyr}}$ ( $\mu\text{M}^{-1} \text{min}^{-1}$ )	$V_{\text{max}}$ ( $\text{min}^{-1}$ )
wild-type TyrH	57 ± 6	87 ± 14	2.2 ± 0.19	1.45	126 ± 4	2.3	1.31	114 ± 10
F300A TyrH	105 ± 5	61 ± 5	0.47 ± 0.02	0.84	51 ± 1	0.45	0.77	47 ± 6
F309A TyrH	63 ± 3	71 ± 10	0.87 ± 0.03	0.79	56 ± 3	2.2	2.0	144 ± 3

<sup>a</sup> The assay measured the formation of dihydroxyphenylalanine from tyrosine as described under Experimental Procedures. The conditions were 100  $\mu\text{g/mL}$  catalase, 10  $\mu\text{M}$  ferrous ammonium sulfate, 50 mM HEPES–NaOH, pH 6.7, at 32 °C. <sup>b</sup> The assay measured the formation of quinonoid dihydropterin from 6-methyltetrahydropterin as described under Experimental Procedures. The conditions were 100  $\mu\text{g/mL}$  catalase, 10  $\mu\text{M}$  ferrous ammonium sulfate, 200  $\mu\text{M}$  NADH, 0.1 unit/mL dihydropteridine reductase, 80 mM HEPES–NaOH, pH 6.7, at 32 °C.

from 37 to 22 °C. The pETYHF309A cultures were incubated at 26 °C. When the  $A_{600}$  value of the cultures reached 0.7–0.8, isopropyl  $\beta$ -D-thiogluconopyranoside (IPTG) was added to a final concentration of 0.25 mM, and incubation was continued for 9.5–15 h. Cells were harvested by centrifugation at 5000g for 30 min and stored at –70 °C overnight.

**Protein Purification.** Wild-type rat TyrH, F300ATyrH, and F309ATyrH were purified as previously described for the wild-type enzyme (12). The purification protocol consists of cell lysis by sonication, polyethyleneimine precipitation, ammonium sulfate precipitation (30–50% saturation for TyrH, 30–42% saturation for F300ATyrH, and 0–35% saturation for F309ATyrH), and heparin–Sephacrose chromatography. For steady-state kinetics, after purification enzymes were dialyzed versus 50 mM Tris–HCl, 10% glycerol, 1  $\mu\text{M}$  leupeptin, 1  $\mu\text{M}$  pepstatin, pH 7.0. Concentrations of proteins were determined using their absorbance at 278 nm (2). Purification of the catalytic domain of TyrH was carried out as described previously (4).

**Assays.** The hydroxylation of tyrosine to form DOPA was measured with a colorimetric end-point assay which determines the amount of DOPA formed (13). Standard conditions for the assay were 50 mM HEPES–NaOH, 100  $\mu\text{g/mL}$  catalase, 10  $\mu\text{M}$  ferrous ammonium sulfate, 250  $\mu\text{M}$  tyrosine, 300  $\mu\text{M}$  6-MPH<sub>4</sub>, pH 6.7, at 32 °C. Assays were carried out for 2 min. For determination of steady-state kinetic parameters, the concentration of 6-MPH<sub>4</sub> was varied from 5 to 500  $\mu\text{M}$ , or the concentration of tyrosine was varied from 5 to 350  $\mu\text{M}$ . Steady-state kinetic data were fit directly to eq 1 using the program Kaleidagraph.

$$v = VS/(K_M + S) \quad (1)$$

Rates of dihydropterin production were determined using a coupled assay with DHPR, monitoring the decrease in absorbance at 340 nm due to NADH oxidation (14). The conditions were 80 mM HEPES–NaOH, 50  $\mu\text{g/mL}$  catalase, 200  $\mu\text{M}$  NADH, 10  $\mu\text{M}$  ferrous ammonium sulfate, 0.2 unit/mL sheep DHPR, pH 6.7, at 32 °C. Because of the difficulty of accurately measuring enzymatic dihydropterin production at high levels of tetrahydropterin due to background autooxidation, the  $V_{\text{max}}$  values for dihydropterin formation were determined by performing assays at 300  $\mu\text{M}$  tyrosine and a concentration of 6-MPH<sub>4</sub> equal to the  $K_M$  value determined with the DOPA formation assay and multiplying the resulting velocity by 2.

**Peptide Analyses.** To determine the effects of excess Fe(II) and 7,8-dihydrobiopterin on the oxidation of amino acid residues in the catalytic subunit and in full-length TyrH, each

enzyme (0.4 mM in 50 mM HEPES at pH 7.0, 0.1 M KCl, and 10% glycerol) was incubated with and without 4 mM 7,8-dihydrobiopterin, 4 mM ferrous ammonium sulfate, and 2.0 mM dithiothreitol (DTT) in a total volume of 100  $\mu\text{L}$  for 48 h at 4 °C, pH 7.0. To each sample was then added 2.5 M urea, 5 mM CaCl<sub>2</sub>, and 0.5 M ammonium bicarbonate buffer, pH 8.0, in a total volume of 0.5 mL, followed by TPCK-treated trypsin to give a ratio of TyrH to trypsin of 50:1 (w/w). The samples were incubated for 12 h at 37 °C; a second aliquot of trypsin was then added and the digestion continued for an additional 6 h. Tryptic peptides were purified by HPLC using a Waters Nova-Pak C<sub>18</sub> column. The chromatography was carried out with 0.05% trifluoroacetic acid for 5 min, followed by a linear gradient over 90 min to 0.045% trifluoroacetic acid 50% acetonitrile, at a flow rate of 1 mL min<sup>–1</sup>. Peptides were collected manually and analyzed by matrix-assisted laser desorption/ionization time-of-flight (MALDI-TOF) mass spectrometry using a Voyager mass spectrometer (PerSeptive Biosystems, Framingham, MA) in the linear positive ion mode with  $\alpha$ -cyano-4-hydroxycinnamic acid as matrix. Fractions containing peptides matching the expected molecular weight were further purified using eluents A and B with a linear gradient from 25% to 50% B over 90 min. Sequences of purified peptides were determined on a Hewlett-Packard G1000A protein sequencer at the Protein Chemistry Laboratory of Texas A&M University.

## RESULTS

**Overexpression and Purification of Mutant Proteins.** The mutant proteins F300ATyrH and F309ATyrH were readily expressed in BL21(DE3) cells, although it was necessary to grow the cells at lower temperatures to avoid accumulation of insoluble enzymes. Both enzymes bound to heparin–Sephacrose and eluted at the same salt concentration as wild-type TyrH, about 0.35 M NaCl. From 1 L of culture we purified 9 mg of F300ATyrH and 7.5 mg of F309ATyrH.

**Steady-State Kinetic Analyses of Mutant Enzymes.** Steady-state kinetic analyses were carried out for each of the purified mutant proteins by measuring separately the rates of formation of the products DOPA and 7,8-dihydropterin. The respective steady-state kinetic parameters appear in Table 1 along with the parameters for the wild-type enzyme. While the two assays gave identical rates with the wild-type enzyme and the F300ATyrH enzyme, with the F309ATyrH enzyme the rate of tetrahydropterin consumption was about 3 times the rate of DOPA formation. The  $K_{\text{Tyr}}$  values for F300ATyrH and F309ATyrH were very similar to that for wild-type TyrH. The  $K_{6\text{-MPH}_4}$  value for F300ATyrH was about twice the wild-



type value, while the  $K_{6\text{-MPH4}}$  value for F309ATyrH was the same as wild-type. The effect of the F300A mutation on the  $V_{\text{max}}$  value was the same for both products; F300ATyrH was approximately 2.5-fold less active than the wild-type enzyme in the production of both DOPA and dihydropterin. The effect of the F309ATyrH mutation on the  $V_{\text{max}}$  value depended upon whether the rate of formation of DOPA or dihydrobipterin was measured. F309ATyrH was 40% as active as the wild-type enzyme in the production of DOPA from tyrosine, but fully active in the production of dihydropterin.

**Characterization of the Hydroxylation Status of Phe300.** Samples of the purified catalytic domain and of the full-length TyrH were analyzed to determine directly if Phe300 is hydroxylated in either enzyme *in vivo*. The expected amino acid sequence of the tryptic peptide containing Phe300 is Asp299-Phe-Leu-Ala-Ser-Leu-Ala-Phe-Arg307. A 40 nmol sample of each protein was digested with TPCK-treated trypsin, and the resulting peptides were separated by HPLC. The HPLC peptide peaks were collected and the molecular masses of the peptide(s) in each peak determined by MALDI-TOF mass spectrometry. A peptide from the catalytic subunit eluting at 51.8 min had a molecular mass of 1039.55, consistent with the expected molecular mass for the Phe300-containing peptide of 1039.56 (Figure 2). Direct amino acid sequencing for five cycles confirmed that the purified peptide contained an unmodified phenylalanine as the second residue (Table 2). The tryptic map of the wild-type protein also showed a peptide eluting at 51.8 min with a molecular mass of 1039.59. The peptide from the wild-type protein was not submitted for amino acid sequence analysis due to the similarity of its HPLC elution profile and molecular mass to the peptide from the catalytic domain.

These results suggested that hydroxylation of Phe300 does not occur during expression of TyrH in *E. coli*, at least under the conditions typically used in this laboratory. However, the proteins used for crystallization were treated with iron and reductant after purification (5). To determine if the crystallization conditions could result in oxidation of Phe300, the above analyses were repeated following the incubation of the catalytic subunit and full-length protein with 4 mM ferrous iron, 4 mM 7,8-dihydrobiopterin, and 2.0 mM DTT for 48 h at 4 °C, the conditions used for crystallization. The catalytic subunit and full-length protein showed a 2-fold decrease in activity following the incubation. The samples were then digested with TPCK-treated trypsin and the peptides separated and collected by HPLC. Both samples showed a peptide eluting at 51.8 min with a molecular mass of 1039.57, as was previously observed in samples of the untreated enzymes. In addition, a new peptide eluting at 50.6 min with a molecular weight of 1055.89 was present in the digest of the catalytic domain (Figure 2). The expected molecular mass for the peptide containing hydroxylated Phe300 is 1055.56. The peptide with mass 1055.89 was purified by HPLC and its amino acid sequence determined. As shown in Table 2, the sequence of this peptide differed from the expected sequence at cycle 2, where a peak eluting at 16.0 min was observed. This did not correspond to the  $R_f$  of any of the standard amino acids. To identify this residue, 3-hydroxyphenylalanine and 2-hydroxyphenylalanine were added to the amino acid standards. 2-Hydroxyphenylalanine standard had a retention time of 16.0 min compared to

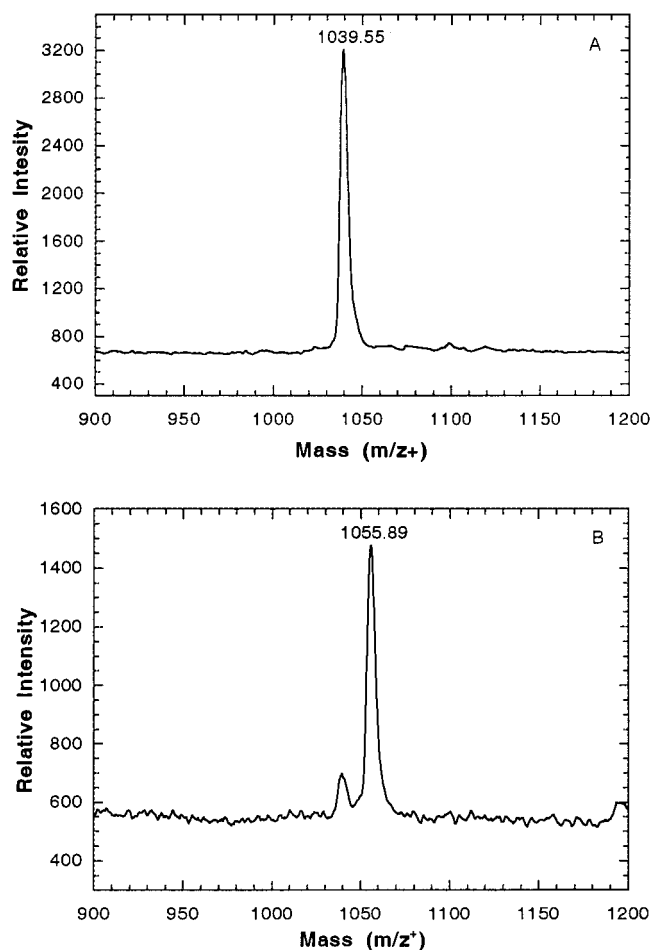


FIGURE 2: MALDI-TOF mass spectrometric analyses of the peptide containing Phe300 from the catalytic domain of TyrH. Peptides were prepared as described under Experimental Procedures. MALDI-TOF mass spectra were acquired in the linear positive ion mode, using  $\alpha$ -cyano-4-hydroxycinnamic acid as the matrix. (A) Mass spectrum of the peptide containing Phe300 from the untreated catalytic domain. (B) Mass spectrum of the peptide containing Phe300 from the catalytic domain treated with 4.0 mM 7,8-dihydrobiopterin, 4.0 mM ferrous ammonium sulfate, and 2.0 mM DTT.

tyrosine (12.1 min) and phenylalanine (18.2 min), while 3-hydroxyphenylalanine had a retention time of 13.5 min. The full-length protein incubated with 7,8-dihydrobiopterin, ferrous iron, and DTT did not yield a peptide with a retention time of 50.6 min. In addition, incubation of the catalytic subunit with excess iron and DTT alone was not enough to generate 2-hydroxyphenylalanine.

## DISCUSSION

The recently described structures of the catalytic domain of TyrH with and without dihydropterin bound have identified active-site residues that may play a role in the catalytic mechanism. Site-directed mutagenesis has provided complementary evidence regarding the roles of several of these residues. The ligands to the iron are His333, His336, and Glu376. Mutation of either histidine residue results in iron-free enzyme with no detectable activity under standard conditions (15). The structure of the 7,8-dihydrobiopterin-bound enzyme suggests that Glu332 is involved in maintaining the correct orientation of the pterin for catalysis. When this residue is replaced with an alanine, the resulting protein

Table 2: Amino Acid Sequences of the Phe300-containing Peptide from the Tryptic Digest of the Catalytic Domain of Tyrosine Hydroxylase

cycle	Phe300-containing peptide without pretreatment		Phe300-containing peptide pretreated with iron, DTT, and 7,8-dihydropterin <sup>b</sup>	
	aa residue	pmol	aa residue	pmol
1	Asp	29.0	Asp	6.9
2	Phe	24.2	XXX <sup>a</sup>	—
3	Leu	15.7	Leu	6.7
4	Ala	21.8	Ala	6.2
5	Ser	5.4	Ser	1.4
6			Leu	5.9
7			Ala	5.7
8			Phe	5.3
9			Arg	3.9

<sup>a</sup> Amino acid residue eluting at 16.0 min corresponding to a 2-hydroxyphenylalanine standard. <sup>b</sup> Pretreated samples were incubated with 4 mM 7,8-dihydrobiopterin, 4 mM ferrous ammonium sulfate, and 2.0 mM DTT in a total volume of 100  $\mu$ L for 2 days at 4 °C, pH 7.0. Pretreated and untreated samples were digested with TPCK-treated trypsin in a 50:1 ratio of TyrH to trypsin, in 2.5 M urea, 5 mM CaCl<sub>2</sub>, and 0.5 M ammonium bicarbonate buffer, pH 8.0, in a total volume of 0.5 mL.

has a 10-fold higher  $K_{6-MPH4}$  value and a 100-fold decrease in the rate of DOPA formation (16), consistent with such a role. In contrast, while Tyr371 has also been proposed to play a role in catalysis (17), replacement of this residue by phenylalanine has no effect on the activity with tyrosine as substrate (18). No structure is yet available with an amino acid substrate bound. Replacement of Arg316 with lysine results in a  $V/K_{Tyr}$  value that is 4000-fold lower than that of wild-type enzyme, while substitution of Asp328 with serine results in an approximately 30-fold increase in the  $K_{Tyr}$  value and a 13-fold lower  $V_{max}$  value for DOPA formation (16). These results implicate Arg316 and Asp328 in binding the amino acid substrate.

Phenylalanine residues at positions 300 and 309 are conserved throughout the family of pterin-dependent hydroxylases. The three-dimensional structure of TyrH with dihydropterin bound showed Phe300 in an aromatic  $\pi$ -stacking interaction with the pterin (6). Remarkably, Phe300 was found to be hydroxylated at the 3-position of the aromatic ring. A similar hydroxylation of Phe300 was also detected in the original ligand-free structure upon reanalysis. The hydroxyl was within hydrogen bonding distance of Gln310, and based upon these results the hydroxyl was proposed to be involved in maintaining the proper orientation of Phe300 for tetrahydropterin binding. No such hydroxylation could be detected for the equivalent phenylalanine residue in the structure of the catalytic domain of PheH, and it was suggested this was due to the different specificities of the two enzymes. The experiments described here were performed to probe the roles of these conserved phenylalanine residues and to determine whether the posttranslational modification of Phe300 is present in vivo.

The steady-state kinetic mechanism of wild-type TyrH has been determined (13). The tetrahydropterin binds first, followed by oxygen and then the amino acid. The rate-limiting step is the reaction with oxygen to form the hydroxylating intermediate (19, 20). With substrates other than tyrosine and with several mutant proteins, the hydrox-

ylating intermediate can break down unproductively (16, 21). This results in an excess of tetrahydropterin being consumed relative to amino acid hydroxylated. Thus, to characterize the effects of a mutant enzyme on catalysis, it is necessary to measure the rates of formation of the two products separately. The primary effect of the F309A mutation is a decrease in the efficiency with which the hydroxylating intermediate reacts with tyrosine to form DOPA. If the rate of tetrahydropterin oxidation alone is measured, this mutant protein has kinetic parameters indistinguishable from those of the wild-type enzyme. These data are consistent with Phe309 playing an indirect role in catalysis by maintaining the proper overall structure of the active site.

For F300ATyrH, the effects on the kinetic parameters were independent of which product was measured. Thus, once the hydroxylating intermediate forms with this enzyme, the reaction proceeds as efficiently as with the wild-type enzyme. There is a decrease in the  $V_{max}$  value of about 2-fold, and this decrease can reasonably be attributed to increased conformational freedom due to the removal of the phenyl ring. This would be expected to result in less optimal orientation of the tetrahydropterin for catalysis. Replacement of the phenyl side chain with a methyl group would still leave a very hydrophobic site, but allow for a somewhat looser fit of the tetrahydropterin. The  $V/K_{6-MPH4}$  value of F300ATyrH is decreased about 5-fold. Since the tetrahydropterin is the first substrate to bind, this  $V/K$  value should only reflect binding interactions. Thus, the primary effect of the mutation of Phe300 to alanine is a decrease in the tetrahydropterin affinity of about 1 kcal/mol, which is comparable to the strength of interactions previously seen between aromatic amino acids and pyrimidines (22). In contrast, mutation of Glu332 in TyrH to alanine decreases the  $V/K_{6-MPH4}$  value about 33-fold (16), while mutation of the homologous residue (Glu286) in PheH results in a 70-fold increase in the  $K_M$  value for tetrahydrobiopterin (3). So while Phe300 does play some small role in maintaining the strength of the interaction of the pterin with TyrH, other residues, such as Glu332, make greater contributions.

The absence of striking effects on binding and catalysis argues against either Phe300 or Phe309 being necessary for activity. They may merely contribute to the optimum shape and position of the active site. Naturally occurring one-base mutations of the codons for Phe300 and Phe309 would result in substitution of leucine, serine, tyrosine, or cysteine. Of these four possibilities, leucine would be the most conservative mutation, substituting a more mobile aliphatic side chain for an aromatic one, but maintaining a hydrophobic environment. The fact that this mutation has not arisen naturally supports the argument that Phe300 and Phe309 help maintain the proper architecture of the active site.

To date no definitive role in the catalytic mechanism has been established for any of the active-site residues of TyrH, so the finding of a hydroxylated Phe300 in crystals of the catalytic domain of TyrH could have major implications for the catalytic mechanism. The posttranslational modification of Phe300 was suggested to occur through a reaction involving Phe300, oxygen, and the enzyme-bound iron (6). The lack of a hydroxylated phenylalanine at the comparable position in PheH raised the possibility that the modified residue is involved in the specificity of these enzymes. In our hands the catalytic domain and full-length TyrH contain

only an unmodified Phe300 when purified. (It should be noted that the catalytic domain utilized here is identical to the protein used in the structural studies.) However, if the catalytic domain is incubated with an excess of ferrous iron, DTT, and 7,8-dihydrobiopterin, similar to the crystal growth conditions, an oxidized Phe300 is found. These results suggest that hydroxylation of Phe300 is not an autocatalytic process necessary for pterin binding but instead only occurs under the conditions used for crystal growth. Similar oxidative damage of proteins has been described for over forty enzyme systems (23). The additional 11–16 amu seen by mass spectrometric analyses of the untreated TyrH described previously could be due to partial oxidation of another amino acid residue or to fractional oxidation of several residues. In addition, there is no solid evidence for the presence of a dihydropterin reductase in *E. coli* that would allow for formation of the tetrahydropterin proposed to be involved in the hydroxylation of Phe300 (24).

Incubation with excess iron, DTT, and pterin only causes modification of Phe300 in the case of the catalytic domain, but not with the full-length enzyme. Previous analyses of the effects of the regulatory domain on the properties of the catalytic domain were interpreted as evidence for increased flexibility of the isolated catalytic domain once the regulatory domain had been removed (4). There would presumably be evolutionary pressure to avoid the adventitious oxidation of active-site residues in TyrH, so that the wild-type enzyme would avoid conformations which would allow such modifications to occur. It is only under the circumstance of the increased conformational flexibility of the active site when the regulatory domain is absent that such a reaction becomes significant.

X-ray crystallography of proteins has proven to be an invaluable tool to elucidate the three-dimensional structure of proteins and provide insights into residues that may play a role in catalysis. There are increasing instances of modified amino acids being identified based upon such structures, e.g., in galactose oxidase (8). This study demonstrates that it is critical to confirm unusual findings obtained from enzyme crystals with data obtained from the enzymes in solution.

## ACKNOWLEDGMENT

We thank Dr. Larry Dangott of the Protein Chemistry Laboratory of Texas A&M University for amino acid sequence analyses and technical assistance.

## REFERENCES

1. Kaufman, S., and Kaufman, E. E. (1985) in *Folates and Pterins* (Blakley, R. L., and Benkovic, S. J., Eds.) Vol. 2, pp 251–352, John Wiley & Sons, New York.
2. Daubner, S. C., Lohse, D. L., and Fitzpatrick, P. F. (1993) *Protein Sci.* 2, 1452–1460.
3. Dickson, P. W., Jennings, I. G., and Cotton, R. G. H. (1994) *J. Biol. Chem.* 269, 20369–20375.
4. Daubner, S. C., Hillas, P. J., and Fitzpatrick, P. F. (1997) *Biochemistry* 36, 11574–11582.
5. Goodwill, K. E., Sabatier, C., Marks, C., Raag, R., Fitzpatrick, P. F., and Stevens, R. C. (1997) *Nat. Struct. Biol.* 4, 578–585.
6. Goodwill, K. E., Sabatier, C., and Stevens, R. C. (1998) *Biochemistry* 37, 13437–13445.
7. Janes, S. M., Mu, D., Wemmer, D., Smith, A. J., Kaur, S., Maltby, D., Burlingame, A. L., and Klinman, J. P. (1990) *Science* 248, 981–987.
8. Ito, N., Phillips, S. E. V., Stevens, C., Ogel, Z. B., McPherson, M. J., Keen, J. N., Yadav, K. D. S., and Knowles, P. F. (1991) *Nature* 350, 87–90.
9. McIntire, W. S., Wemmer, D. E., Chistoserdov, A., and Lidstrom, M. E. (1991) *Science* 252, 817–824.
10. Mager, H. I. X., Addink, R., and Berends, W. (1967) *Recl. Trav. Chim. Pays-Bas* 86, 833–850.
11. Kunkel, T. A., Roberts, J. D., and Zakour, R. A. (1987) *Methods Enzymol.* 154, 367–380.
12. Daubner, S. C., Lauriano, C., Haycock, J. W., and Fitzpatrick, P. F. (1992) *J. Biol. Chem.* 267, 12639–12646.
13. Fitzpatrick, P. F. (1991) *Biochemistry* 30, 3658–3662.
14. Dix, T. A., and Benkovic, S. J. (1985) *Biochemistry* 24, 5839–5846.
15. Ramsey, A. J., Daubner, S. C., Ehrlich, J. I., and Fitzpatrick, P. F. (1995) *Protein Sci.* 4, 2082–2086.
16. Daubner, S. C., and Fitzpatrick, P. F. (1999) *Biochemistry* 38, 4448–4454.
17. Erlandsen, H., Fusetti, F., Martinez, A., Hough, E., Flatmark, T., and Stevens, R. C. (1997) *Nat. Struct. Biol.* 4, 995–1000.
18. Daubner, S. C., and Fitzpatrick, P. F. (1998) *Biochemistry* 37, 16440–16444.
19. Fitzpatrick, P. F. (1991) *Biochemistry* 30, 6386–6391.
20. Francisco, W. A., Tian, G., Fitzpatrick, P. F., and Klinman, J. P. (1998) *J. Am. Chem. Soc.* 120, 4057–4062.
21. Hillas, P. J., and Fitzpatrick, P. F. (1996) *Biochemistry* 35, 6969–6975.
22. Shamoo, Y., Ghosaini, L. R., Keating, K. M., Williams, K. R., Sturtevant, J. M., and Konigsberg, W. H. (1989) *Biochemistry* 28, 7409–7417.
23. Stadtman, E. R. (1990) *Free Radical Biol. Med.* 9, 315–325.
24. Eschenbrenner, M., Coves, J., and Fontcave, M. (1995) *FEBS Lett.* 374, 82–84.

BI991160U